IOSR Journal of Mechanical and Civil Engineering (IOSR-JMCE)
e-ISSN: 2278-1684,p-ISSN: 2320-334X, Volume 15, Issue 3 Ver. I (May. - June. 2018), PP 29-37
www.iosrjournals.org

Milling Parameter Optimization For The Manufacture of Sub-Micrometric Portland Cement

G. M. Rodríguez-Torres[1], J. Zárate-Medina[2], J. C. Rubio Ávalos[3], J. A. Rodríguez-Torres[4], M. E. Contreras García[5]

[1,2,4 & 5]*Instituto de Investigación en Metalurgia y Materiales, Universidad Michoacana de San Nicolás de Hidalgo, C.U. Edificio U, C.P. 58040, Morelia, Michoacán, México*
[3]*Facultad de Ingeniería Civil, Universidad Michoacana de San Nicolás de Hidalgo, C.U. Edificio C, C.P. 58040, Morelia, Michoacán, México*
Corresponding Author: G. M. Rodríguez-Torres

Abstract : *Today, ultra-high-performance nanostructured concrete is being developed by using high-fineness Portland cement with blast furnace nano-slag and other nanomaterials. The primary aim of this research was to obtain the optimum milling parameters of Portland cement with an average particle size (APS) in the submicron range, by using a planetary ball mill with 5/8" and 1/2" ball diameters. The Portland cement was subjected to different grinding processes, varying the combination of the parameters, until obtaining an APS in the submicron range. The characterization for both the as-received and milled Portland cement was carried out through the following techniques: laser diffraction, XRD, scanning electron microscopy, specific surface area of the cement, and normal cement consistency. The optimum milling parameters were then analyzed and evaluated. The average particle size of the submicron Portland cement obtained through the optimal combination of the parameters was 0.84 μm*

Keywords: *Portland cement; average particle size; planetary ball mill; milling parameters*

Date of Submission: 26-04-2018 Date of acceptance: 14-05-2018

I. Introduction

Various applications have been proposed by different authors for the development of composite materials using very fine Portland cement. They include thin coatings with high adhesion, clean concrete, and nanoparticle-reinforced composites, with a consequent improvement in endurance and the compatibility of cement with different nano-materials, such as nano tubes and nano-silica, among others [1]. Currently, many researchers have turned their attention to the development of concrete based on Portland cement with enhanced features, by adding nanoparticles of different physical and chemical characteristics, resulting in improved strength and durability. [2-4]. A reduced average particle size generally results in an increase in the rate of hydration, as well as improved mechanical properties, such as early-age resistance [5], but drying shrinkage also increases due to the increased hydration heat. Juan Carlos Arteaga-Arcos et al. [6] found that by partially replacing cement containing normal-sized particles with ultrafine cement (a particle size under 11 μm), compressive strength increased. Other authors used cement that was ground to nano-metric-sized particles and concluded that the initial setting time was substantially decreased, compared with cement with normal-sized particles [7]. The increase in the specific surface area of more than 7000 cm2/g, calculated by the Blaine procedure, resulted in a decline in later-age resistance and in a faster setting time [8]. In addition, by mixing ultrafine cement with nano-furnace slag, it was possible to obtain ultra-high-performance concrete [n].

There are two different ways to obtain fine cement: by dry milling and by wet milling. Cement obtained through dry milling has a high fineness with a maximum particle size under 20 μm [9]. On the other hand, Byung-Wan Jo et al. [10] obtained very high fineness cement using the bead milling process, achieving a particle size of approximately 220 nm, starting from a microscale particle of approximately 12.57 μm, using methanol and ethanol as dispersing agents. Zhichu Huang et al. [11] obtained fine cement with a maximum particle size under 40 μm through the wet milling method. However, because the cement is subjected to a wet milling process with water, the resulting slurry must be used as rapidly as possible. N. Bouzoubaa et al. [12] achieved a greater specific area through a mixture of large and medium grinding ball sizes that progressively increased with the milling time. New tendencies for obtaining high-performance cement (HPC) using different nanoparticles [9, 11, and 12] require the formulation of those new composites, so that there is greater size coherency between the nanoparticles. The nanoparticles will act as the reinforcement and hydration products of the cement and, in turn, will become the matrix. In addition to improving the cement paste by adding nanosized particles, there can be an even bigger contribution if finer cement is used. Consequently, cement particles will

have better interaction and a homogeneous nanoparticle distribution. This was the motivation for conducting the present research that produced submicron-sized cement at the laboratory level.

II. Experimental Procedure

2.1 Materials and Equipment

A commercially available Mexican Standard NMX-C-414-0NNCCE-2014 Portland-composite cement CPC 40 [13] (fig 1) (table 1) was used. This kind of cement is comparable to the European Standard EN 197-1 Portland-composite cement CEM II/B-M [14]. It was subjected to the grinding process, using a RETSCH model PM 100 Planetary ball mill with a maximum volume capacity of 500 ml, a speed of 650 RPM, and the possibility of two-direction rotation. Both the vial and the grinding media were stainless steel and 5/8" and 1/2" balls were used as the grinding media. The main characteristics of the commercial cement are shown in Table 1.

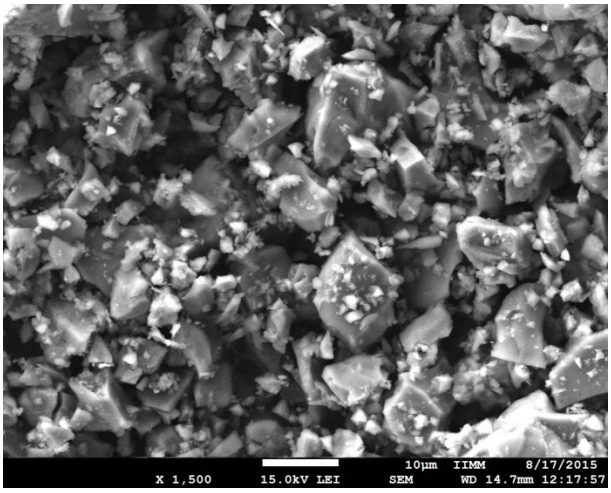

Figure 1. As-received CPC 40 cement.

Table 1. Starting Portland cement CPC 40 properties (average values of two tests).

Density g/cm^3	BET specific surface area (SSA) cm^2/g	APS (µm)	Maximum Particle Size µm	Normal consistency %
3.13	17180	13.45	40	26.45

The mineralogic identification of cement was carried out using the x-ray diffraction technique (XRD) in a Bruker D8 ADVANCE DAVINCHI model with CuK radiation. The analysis was done with monochromatic radiation in a graphite monochromator, scanning from 20 to 85 degrees (2θ), a step size of 0.02 degrees, and a step with continuous time of 0.06 seconds. The average particle size (APS) of all the cements was measured in 100Q LS BECKMAN COULTER equipment, applying the laser diffraction principle, which assumes that the particles are spherical, and verifying the data through scanning electron microscopy (SEM). According to the literature, this technique provides acceptable results [15] in the dry process. The sample was placed in an oven at 105°C for one hour before undergoing the test. SEM image analysis was performed using LINCE software. More than 600 particles were measured in each SEM image, obtaining the average particle size through a statistical data process. Particle agglomeration for the different grinding processes was analyzed by SEM, using a field emission scanning electron microscopy (FESEM) technique, with a JEOL JSM 7600F microscope. Specific surface area was determined by the BET method, employing a Quantasorb Jr. analyzer (QUANTACHROME CORP.), which allows nitrogen adsorption at a liquid nitrogen temperature in a dynamic flow mode [15]. This technique was applied to the submicronic-sized cement, obtained through the combination of optimal parameters and compared with the Portland cement CPC40 control sample.

2.2 Grinding process.

Considering the initial size of the grinding media as a constant (1/2 "diameter), three factors that significantly influence the grinding process were considered in the present study: Factor A: the ball-to-sample ratio (b/s), Factor B: milling speed (rpm), and Factor C: milling time (h). In this experimental process, two intensity levels, high (+) and low (-), were assigned to each factor. Therefore, the initial matrix determining the number of combinations between the grinding parameters in the present research was Rk, where R represents the number of intensity levels taken by each factor (2 in this case), and k the number of factors involved (k = 3). The low levels (-) were: A = 3/1, B = 200 rpm, and C = 1 hour. The high levels (+) were: A = 10/1, B = 500

rpm, and C = 6 hours. The combinations of the factors for each experiment and the corresponding sample level are shown in table 2. The eight milling processes were performed by dry milling. Once all initial combinations were evaluated, the factors that had the greatest effects on milling were identified and new combinations were made. A combination of ball milling media diameters of 1/2"and 5/8" was also included. In the final milling processes, a few drops of isopropyl alcohol (1.5ml/255g) as a dispersing agent were added to avoid the agglomeration that presented in the initial tests.

The rotation direction of the vial was changed every hour and the grinding was interrupted for five minutes to avoid vial overheating. As a result, the total grinding time for the high level was 6 hours and 30 minutes. The sample was then placed in an oven at 100°C to remove all residual alcohol, after which it was characterized by XRD, laser diffraction, and SEM, verifying the composition, APS, and agglomeration.

Table 2. 2^3 Experimental design matrix for the milling parameters with a grinding media diameter of ½".

Sample weight (g)	Sample ID	A (b/s ratio)	B (h)	C (rpm)
55.00	PC1	3/1(-)	1 (-)	200 (-)
16.50	PC2	10/1(+)	1(-)	200 (-)
55.00	PC3	3/1(-)	6(+)	200 (-)
16.50	PC4	10/1(+)	6(+)	200 (-)
55.00	PC5	3/1(-)	1(-)	500 (+)
16.50	PC6	10/1(+)	1(-)	500 (+)
55.00	PC7	3/1(-)	6(+)	500 (+)
16.50	PC8	10/1(+)	6(+)	500 (+)

2.3 Normal Consistency of the as-received CPC 40 cement and the submicron cement

Finally, the normal consistency of the cement was evaluated in both CPC 40 as obtained from the supplier and the cement obtained after the grinding process with submicron APS, to evaluate the influence of APS on water consumption. The Vicat apparatus was used to perform the analysis and the procedures were carried out according to norm ASTM C 187 [16].

2.4 Power consumed by the grinding equipment

The energy consumed by the grinding equipment (PBM) for each milling process that produced the submicron particle size was also evaluated. A NanoVIP PLUS power and harmonic analyzer was used to measure the power.

III. Results And Discussion

3.1. Average particle size (APS)

To evaluate the effect of different milling parameters as a function of milling time (B) for the samples defined in Table 2, the APS was related to the milling time (B) in figure 2 of each combination. Figure 2 shows that for samples PC4, PC7, and PC8, the APS grew. However, for the PC3 sample, the APS continued to decrease until reaching the size of 1.5 μm when the milling time was increased to 8 hours. After 10 hours of grinding, it then increased to 2.44 microns. Those results suggest that when the PC1 sample was submitted to the lower energy and the PC8 sample was submitted to the higher energy, particle agglomeration increased in that same order. This can be explained in terms of the ability of particles to agglomerate. Agglomeration increases when particle size is reduced, absorbing energy through agglomerate volume deformation, thereby decreasing the net energy for the fracturing of each individual particle. The PC1 and PC3 sample curves in Fig. 2, relating APS to milling time, represent the nearly optimal milling process for producing the submicron particle size, with no agglomeration during the process. This is consistent with that described above, given that it is the lower induced energy curve. However, the cost of obtaining low agglomeration in the dry milling process is the long length of time required for milling.

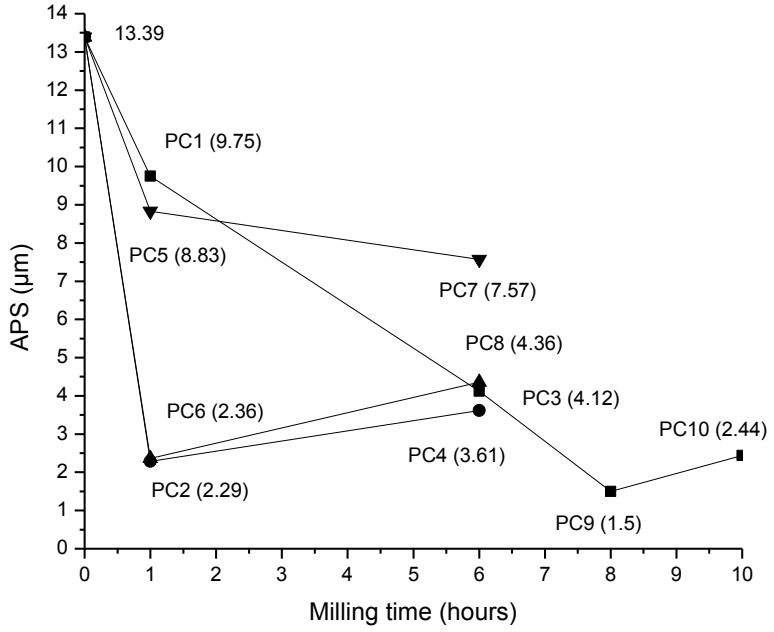

Figure 2. Variation of APS as a function of milling time.

The PC6 and PC8 samples are the ones with the highest degree of agglomeration, which is due to the high energy produced by the high speed and dry condition of the milling process. Under those conditions, particle agglomerates are formed and adhere to the walls of the vial and the grinding media. Only loose particles are recovered, with very low yielding. The agglomerates formed are clearly distinguishable through SEM observation of the agglomerated material in the vial walls (Fig. 3). In those grinding processes, the temperature becomes too high, due to the high energy produced, making it impossible to continuously maintain the milling process. In addition, long periods of time are required to cool the vial.

3.2 SEM analysis

The PC1 sample curve in Fig. 2 shows that the agglomeration was small throughout the 10-hour process, which was corroborated by SEM (Fig. 4a), achieving an APS of 2.44 µm. However, in the same micrograph, there are very large particles (up to 15 µm), indicating that the grinding media acted mainly on the small particles, with very little fracturing of the large ones. Bimodal particle size distribution, as shown in Fig. 5, indicates that larger grinding media are required to act on the larger particles of the sample. This is consistent with the results presented by Seyfý Erdem et al. [17], who found that the particle size of the sample maintains a very strong relationship with respect to the particle size of the grinding media. In the present study, small grinding media particles (1/2") were incapable of fracturing the large particles of the sample, hence the average particle size limited the continuous decrease in size. Therefore, the decision was made to submit Portland cement CPC40 to a longer grinding process (8h and 10h). Those samples were labeled PC9 and PC10, respectively, maintaining the same factor combination (3/1-200). In this manner, the two extra APS values obtained were graphed in Figure 2, showing that at 8h, the APS continued to decrease to 1.5 µm, but with 10h of grinding, the particles agglomerated, raising the APS value to 2.44 µm. In addition, larger milling media (5/8") were used to obtain better results. The larger particles were ground more easily with 10h, but hard agglomerates were obtained in the vial walls and in the grinding media (Fig. 4b), with low recovering of the material.

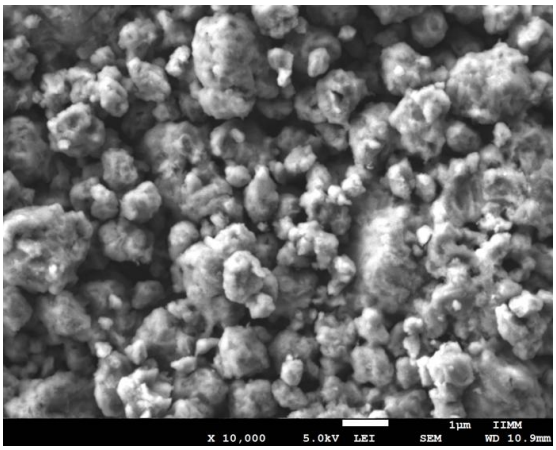

Figure 3. PC7 agglomerated particle sample.

Based on our results, other milling processes were performed using PC12 combinations (3/1-5-200), i.e. keeping the b/s ratio and milling speed, but decreasing the milling time with a sample weight of 107g. Combined milling media sizes of 5/8" and 1/2" and 1.0ml of isopropyl alcohol as a dispersing agent were also used, achieving an APS = 0.94 µm, as shown in Fig. 6. According to the equation described by Nedeljko Magdalinovic et al. [18], the diameter size of the milling media is directly proportional to the diameter of the particles to be ground, which indicates that if the sample has a known particle size distribution before subjecting it to milling, the milling media should also have a similar particle size distribution. According to the theoretic hypothesis of those authors, if the form of the size distribution curve of the milling media were similar to the size distribution of the particles to be ground, the grinding process would be more efficient. Finally, the working capacity of the Lab Mill Unit recommended by the manufacturer is 80% of its volume, including the sample and the grinding media, and the 500-ml volume of the vial was also considered. Based on the analysis of the volume ratios of the respective materials, the sample size was adjusted to the 255-g maximum capacity of the mill. Thus, the grinding process was carried out increasing the milling rate from 200 rpm to 250 rpm, while keeping the remaining two parameters the same (b/s ratio of 3/1 and milling time of 5 hours), consequently maintaining the APS at 0.84 µm, as shown in Fig 7.

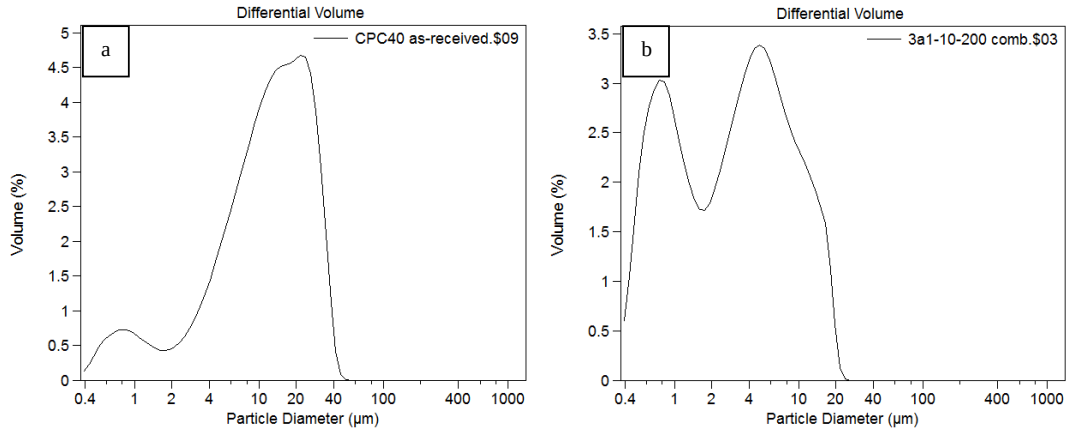

Fig. 5. Differential volume from the laser diffraction technique: a) as-received CPC 40 and b) PC10 and ball diameter of ½".

3.3 Specific surface area (SSA) by the BET method.

The BET analysis was performed on both the sample obtained with the grinding process that produced the submicronic APS (3/1-5-250) PC13 and the control cement. The results are presented in Table 3 and show that the SSA of the sample obtained through the low-speed grinding process at 250 rpm had a 76% increase in SSA, compared with the control sample. The particle size distribution obtained for the PC13 sample was determined through SEM image analysis (Figure 8), finding a wider particle size distribution in the PC13 sample than in the control cement. The distribution was: 10% of particles smaller than 0.40 µm, 45.35% of particles smaller than 1.00 µm, and 91.92% of particles smaller than 3.60 µm. The maximum size was 14.10 µm, representing only 1.38% of the sample. For the statistical analysis of each image, 600 measurements of particle diameter were considered.

Table 3 Specific surface area, average particle size, and normal consistency of control and submicron Portland cements.

Sample	Isopropyl alcohol	SSA by BET (m^2/gr)	APS (µm)	Normal Consistency % water
CPC 40 Control	--	1.718	13.45	26.45
PC7 (5/8" y ½")	2.0ml/255g CPC40	3.453	Agglomerated	41.60
PC13 (5/8" y ½")	1.5ml/255g CPC40	3.018	0.84	39.50

3.4 X-Ray Diffraction

Fig. 9 shows the x-ray diffraction patterns of the as-received Portland cement CPC 40, agglomerated sample, PC7, and the optimal combination of the parameters PC13. The phases present were: tricalcium aluminate C3A (C), tricalcium silicate C3S (A), dicalcium silicate C2S (B), calcium carbonate CaCO3 (D), calcium sulfate CaSO4 (S), and tetra calcium aluminoferrite C4AF (F), in concordance with Stutzman PE et al. [19]. As the energy supplied to the sample increased during the grinding process, there was a broadening of the peaks and a decrease in their intensity, as shown in Figure 9, especially in the insert showing the detail of the alite peak. This is due to a decreasing in the crystallite size and the amorphization of different phases embedded into the sample induced by the grinding process and is consistent with the findings of Juan Carlos Arteaga-Arcos et al. [6], A. Hamouda et al. [20], and Konstantin Sobolev et al. [21]. There may be differences in the degree of amorphism between the mineral phases in the Portland-composite cement CPC 40 subjected to a grinding process, which are possibly because of the difference in toughness of the phases. For the grinding process with the optimum combination of PC13 parameters (3/1-5-250), there was little influence on the decrease in intensity and amplification of the peaks in the diffraction pattern because the magnitude of the parameters was small, indicating low milling energy in the process, thus reducing the agglomeration of the particles (Figure 9) and the temperature in the vial.

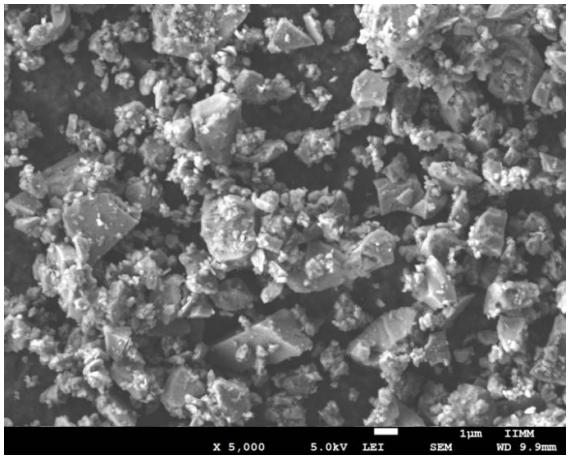

Figure 6. SEM image of the PC12 sample with mixed ball diameters of 5/8" and 1/2" with 1.0ml of isopropyl alcohol (sample weight of 107g).

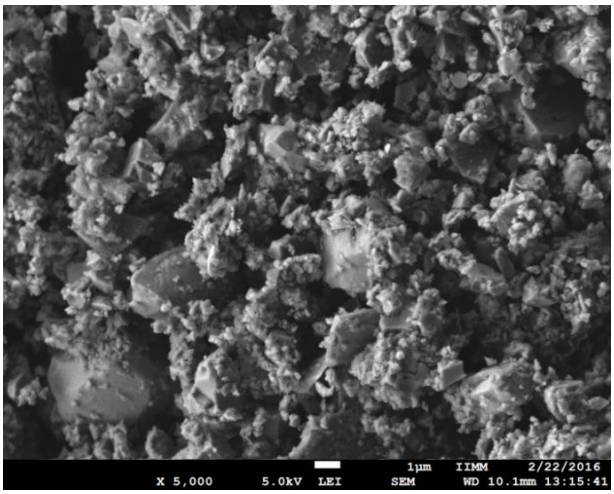

Figure 7. SEM image of the PC13 sample with mixed ball diameters of 5/8" and 1/2" with 1.5ml of isopropyl alcohol (sample weight of 255g).

3.5 Normal consistency of the cements

Since setting time is one of the properties most affected by increasing the fineness of cement, namely, reduced setting time [04], in the present work, the normal consistency of the control cement was determined, as well as that of the submicron cement, according to ASTM C 187-11E1 cement [16]. Table 3 presents the test results of the control and the two submicron cements. The amount of water required to give the cement normal consistency increased substantially from 26.45%, to 39.50%, and to 41.60%. Finally, the increment of SSA induced by the grinding process was associated with the increase of water required to obtain normal consistency and the consequent reduction of the initial setting time.

3.6 Equipment power consumption

Table 4 shows that by increasing the speed of the process, the grinding time required to obtain specific superficial area greater than 3 gr/m^2 was decreased. However, the power required by the equipment was also increased. Thus, the total energy consumed (KWH) by the equipment throughout the process was obtained by multiplying the power required by the milling time. The same table shows that the process that required less energy to obtain the desired APS, was the one corresponding to the speed of 250 RPM.

Table 4. Energy consumed by two different grinding processes to obtain submicron average particle size

Speed (RPM)	Power (W)	SSA by BET (m^2/gr)	Grinding time (H)	Energy consumed (KWH)
250	180	3.018	5	0.9
500	616	3.453	3	1.848

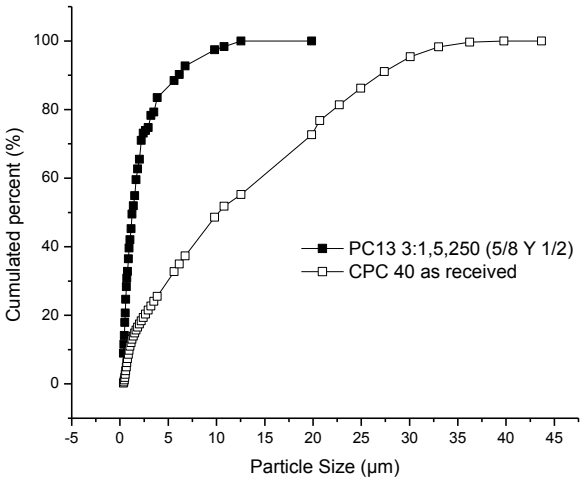

Figure 8. Particle size distribution measured for as-received CPC 40 and that obtained by optimum parameters (PC13).

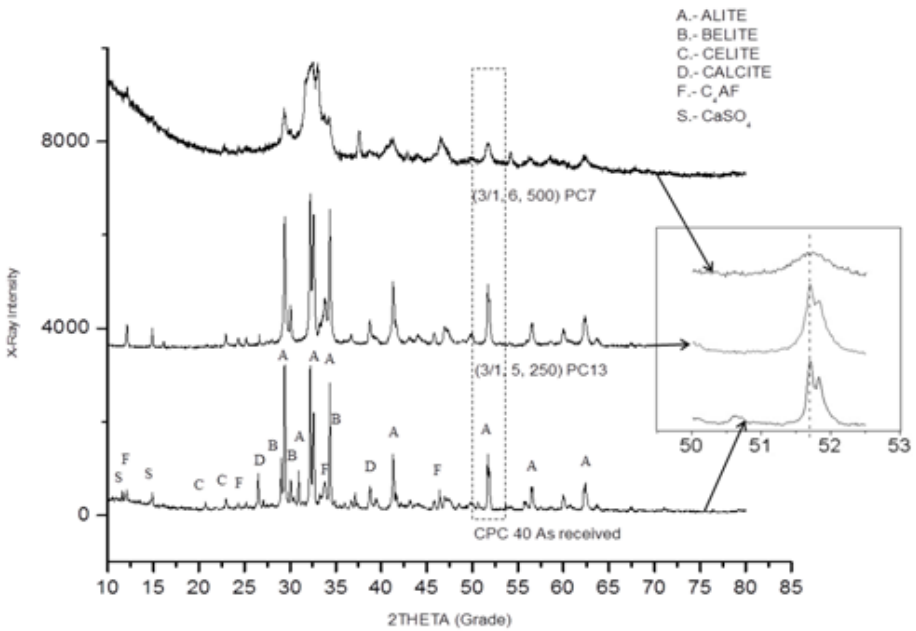

Figure 9. Evolution of x-ray diffraction patterns as a function of the milling process.

IV. Conclusion

Particle size distribution of the CPC 40 cement was modified by changing the milling conditions, decreasing from 13.45-micron APS to 0.84 microns, with a maximum particle size of 14.10 μm. This represented only 1.38% of the sample and was carried out using a planetary ball mill at the laboratory level. The optimum parameter combination was: a 3:1 ball-to-sample ratio, a milling speed of 250 rpm, a milling time of 5 hours, mixing the 5/8" and 1/2" ball diameters (2:1 ratio), the dry process, plus the addition of only 1.5ml of isopropyl alcohol per 255 g of CPC 40, all of which were very beneficial for obtaining the smallest particle size distribution. From the results of the XRD analysis, it was concluded that as the milling energy increased in the samples, the degree of amorphism of the material also increased. However, the diffraction patterns showed that with the optimum combination of grinding parameters, the broadening of the peaks and the decrease in their intensity were small, indicating that the degree of amorphism was also small. Finally, it is important to conduct studies of setting time and mechanical property evolution with respect to time to evaluate the effect of the high SSA of cements subjected to high-energy grinding processes, given that they represent cements with mechanical activation.

Acknowledgements

The authors acknowledge the financial support for this research provided by the Consejo Nacional de Ciencia y Tecnología (CONACYT) and CIC-UMSNH and G. M. Rodríguez – Torres acknowledges to CONACyT for doctoral scholarship.

References

[1] Perumalsamy Balaguru and Ken Chong, Nanotechnology and concrete: research opportunities. *National Science Foundation, USA. Proceedings of ACI Session on "Nanotechnology of Concrete: Recent developments and Future Perspectives" November 7,* 2006, Denver, USA pp. 15-28.

[2] Ye Qing, Zhang Zenan, Kong Deyu, Chen Rongshen, Influence of nano-SiO2 addition on properties of hardened cement paste as compared with silica fume. *Construction and Building materials Vol 21*, 2007, pp. 539-545. doi:10.1016/j.conbuildmat.2005.09.001.

[3] Xiaoyan Liu, Lei Chen, Aihua Liu, Xinrui Wang, Effect of Nano-CaCO3 on Properties of Cement Paste. *International Conference on Future Energy, Environment, and Materials. SciVerse ScienceDirect Energy Procedia Vol 16*, 2012, pp. 991-996. doi:10.1016/j.egypro.2012.01.158

[4] L. Senff, D. Hotzab, S. Lucas, V.M. Ferreira, J.A. Labrincha, Effect of nano-SiO2 and nano-TiO2 addition on the rheological behavior and thehardened properties of cement mortars. *Materials Science and Engineering A. SciVerse ScienceDirect. Vol 532,* 2012, pp. 354-361. doi:10.1016/j.msea.2011.10.102

[5] Dale P. Bentz, Edward J. Garboczi, Claus J. Haecker, Ole M. Jensen, Effects of cement particle size distribution on performance properties of Portland cement-based materials. *Cement and Concrete Research. Vol. 29,* 1999, pp. 1663-1671.

[6] Juan Carlos Arteaga-Arcos, Obed Arnoldo Chimal-Valencia, Hernani Tiago Yee-Madeira, Sebastián Díaz de la Torre, The usage of ultra-fine cement as an admixture to increase the compressive strength of Portland cement mortars. *Construction and Building Materials. Vol 42,* 2013, pp. 152-160. doi.org/10.1016/j.conbuildmat.2013.01.017.

[7] Parang Sabdono, Frisky Sustiawan, Dion Aji Fadlillah, The effect of nano-cement content to the compressive strength of mortar. *Procedia Engineering. Vol 95*, 2014, pp 386-395. doi: 10.1016/j.proeng.2014.12.197.
[8] Shondeep L. Sarkar, John Wheeler, Important properties of an ultrafine cement - Part I. *Cement and Concrete Research. Vol 31*, 2001, pp. 119-123.
[9] Juan Carlos Arteaga-Arcos, Obed Arnoldo Chimal-Valencia, David Joaquin Delgado, Hernani Tiago Yee-Madeira, Sebastián Díaz de la Torre, High energy ball mill parameters used to obtain ultra-fine Portland cement at laboratory level. *ACI Materials Journal. Vol 108 No. 4*, 2011, pp. 371-377.
[10] Byung-Wan Jo, Sumit Chakraborty, Ki Heon Kim, and Yun Sung Lee, Effectiveness of the Top-Down Nanotechnology in the Production of Ultrafine Cement (~220 nm). *Hindawi Publishing Corporation. Journal of Nanomaterials. Volume 2014,* pp 1-9. doi.org/10.1155/2014/131627.
[11] Zhichu Huang, Mingxiang Chen, Xurong Chen, A developed technology for wet-ground fine cement slurry with its applications. *Cement and Concrete Research volume 33*, 2003, pp. 729–732. doi:10.1016/S0008-8846(02)01035-9.
[12] N. Bouzoubaa, M.H. Zhang, A. Bilodeau, and V.M. Malhotra, The effect of grinding on the physical properties of fly ashes and a portland cement clinker. *Cement and Concrete Research. Vol. 27, No. 12*, 1997, pp. 1861 – 1874.
[13] Norma Mexicana NMX-C-414-ONNCCE-2014. *Industria de la Construcción – Cementantes Hidráulicos – Especificaciones y Métodos de Ensayo*. 17 pp.
[14] DIN EN 197-1 Standard Cement - Part 1: Composition, specifications and conformity criteria for common cements. 2011-11
[15] Chiara Ferraris and Edward Garboczi, Digest by Haleh Azari, Responsible Senior Program Officer: E. T. Harrigan, Measuring Cement Particle Size and Surface Area by Laser Diffraction. *National Cooperative Highway Research Program, National Academies of Science. April*, 2013, pp. 1-11.

G. M. Rodríguez-Torres. Milling Parameter Optimization For The Manufacture of Sub-Micrometric Portland Cement ." IOSR Journal of Mechanical and Civil Engineering (IOSR-JMCE) , vol. 15, no. 3, 2018, pp. 29-37